

Floquet control of global PT symmetry in 2D arrays of quadrimer waveguides

Bo Zhu,^{1,2} Honghua Zhong,^{1,3,*} Jun Jia,⁴ Fuqiu Ye,⁴ and Libin Fu^{3,†}

¹*Institute of Mathematics and Physics, Central South University of Forestry and Technology, Changsha 410004, China*

²*School of Physics and Astronomy, Sun Yat-Sen University (Zhuhai Campus), Zhuhai 519082, China*

³*Graduate School, China Academy of Engineering Physics, Beijing 100193, China*

⁴*Department of Physics, Jishou University, Jishou 416000, China*

(Dated: March 13, 2024)

Manipulating the global PT symmetry of a non-Hermitian composite system is a rather significant and challenging task. Here, we investigate Floquet control of global PT symmetry in 2D arrays of quadrimer waveguides with transverse periodic structure along x -axis and longitudinal periodic modulation along z -axis. For unmodulated case with inhomogeneous inter- and intra-quadrimer coupling strength $\kappa_1 \neq \kappa$, in addition to conventional global PT -symmetric phase and PT -symmetry-breaking phase, we find that there is exotic phase where global PT symmetry is broken under open boundary condition, whereas it still is unbroken under periodical boundary condition. The boundary of phase is analytically given as $\kappa_1 \geq \kappa + \sqrt{2}$ and $1 \leq \gamma \leq 2$, where there exists a pair of zero-energy edge states with purely imaginary energy eigenvalues localized at the left boundary, whereas other $4N - 2$ eigenvalues are real. Especially, the domain of the exotic phase can be manipulated narrow and even disappeared by tuning modulation parameter. More interestingly, whether or not the array has initial global PT symmetry, periodic modulation not only can restore the broken global PT symmetry, but also can control it by tuning modulation amplitude. Therefore, the global property of transverse periodic structure of such a 2D array can be manipulated by only tuning modulation amplitude of longitudinal periodic modulation.

I. INTRODUCTION

Global parity-time (PT) symmetry plays a key role in determining the real energy spectrum, topological character and transport property of non-Hermitian composite system [1–8]. There are many interesting physical phenomena related to global PT symmetry, including topological bound state [9], edge-mode lasing [10], anomalous edge states [11] and anisotropic transmission resonances [12]. A characteristic property of global PT -symmetric system is the existence of a phase transition (spontaneous global PT -symmetry-breaking) from the unbroken to broken- PT -symmetric phase whenever the gain/loss parameter exceeds a certain threshold. This has been experimentally demonstrated in synthetic photonic lattices [9, 13] and cavity laser arrays [14]. Therefore, an important issue in a global PT -symmetric system is the ability to control and tune this phase transition.

Optical structures constructed by arrays of coupled dimers [15–23], trimer [24] or quadrimer [25–27], provide a fertile ground to observe and utilize notions of global PT symmetry. Global PT symmetry of such system will require precise relation between various on-site energies and coupling symmetry between the building blocks, and hence becomes extremely fragile in the presence of disorder, impurities and boundaries which can support localized modes [28–33]. One of the most significant features of such optical structure is the boundary condition dependence, where system under periodic boundary condition (PBC) and open boundary condi-

tion (OBC) have dramatically different energy spectra, and the zero-energy edge states (topologically nontrivial phase) related to spontaneous global PT -symmetry-breaking transition can appear. These have received great research interests in a class of photonic arrays of PT -symmetric dimers described by the non-Hermitian Su-Schrieffer-Heeger (SSH) model [34–38]. It was shown that there is no universal correlation between spontaneously global PT -symmetry-breaking and the topologically nontrivial phase, and only the symmetry of the individual edge states can decide whether their presence has an influence on the global PT symmetry [35]. Thus the key outstanding question is: What is the accurate parametric region of the boundary influencing global PT symmetry?

Recently, based on the high-frequency Floquet method to rescale the coupling strength, periodic modulations have been proposed to control PT symmetry of single optical dimer [39–46]. It has been found that manipulation of PT -phase transition can be achieved by adjusting modulation parameter. The Floquet PT -symmetric system also has been realized for two coupled LC resonators with balanced gain and loss [47]. However, these previous works mainly consider that out-of-phase periodic modulations were introduced on complex on-site energies or intra-dimer coupling strength. This is a rather challenging task in optical experiment, as the balanced gain and loss and periodic modulation in the complex refractive index must be tuned simultaneously. Therefore, the protocol that the additional modulated dimer is introduced to constitute a periodically modulated PT -symmetric quadrimer may be more easily operate in experiment. Especially, the study on Floquet control of global PT symmetry in such a composite array is still

* hhzhong115@163.com

† lbfu@gscaep.ac.cn

lacking.

In this work, we address above these important questions by investigating global PT symmetry and its Floquet control in 2D arrays of quadrimer waveguides with transverse periodic structure along x -axis and longitudinal periodic modulation along z -axis, whose single quadrimer is coupled by a PT -symmetric dimer and a periodically modulated dimer. Our main results are:

i) There exists an exotic phase where global PT symmetry is broken under OBC, whereas it still is unbroken under PBC for unmodulated case with asymmetric coupling between inter- and intra- quadrimer. The boundary of phase is analytically given as $\kappa_1 \geq \kappa + \sqrt{2}$ and $1 \leq \gamma \leq 2$, where there exists a pair of zero-energy edge states with purely imaginary energy eigenvalues localized at the left boundary, whereas other $4N - 2$ eigenvalues are real.

ii) The system may support the triple point, where three phases of robust global- PT -symmetry (RPT), boundary influencing global- PT -symmetry (BIPT), and broken global- PT -symmetry (BPT) touch. Thus depending on how parameters change in vicinity of the triple point, breaking of global PT symmetry can occur in two different ways: RPT \rightarrow BPT, or RPT \rightarrow BIPT \rightarrow BPT.

iii) The domain of the exotic phase can be manipulated narrow and even disappeared by tuning modulation parameter A/ω . More interestingly, whether or not the array has initial global PT symmetry, periodic modulation not only can restore the broken global PT symmetry, but also can control it by tuning modulation amplitude.

iv) The global property of transverse periodic structure of such a 2D array can be manipulated by only tuning modulation amplitude of longitudinal periodic modulation, which provides a promising approach for designing and manipulating optical material and may has specific technological importance.

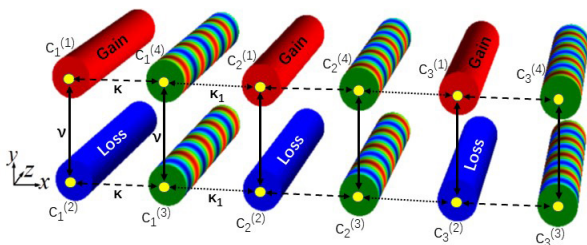


Figure 1. (Color online) Schematic diagram of a 2D waveguide array comprised by periodically modulated PT -symmetric quadrimers. The periodic change of color along the z -axis denotes the periodic modulation $A\sin(\omega z)$. The intra-dimer coupling strength ν is tuned by adjusting the center-to-center waveguide spacing along y -axis Δy ; the intra-quadrimer coupling strength κ and the inter-quadrimer coupling strength κ_1 are tuned by intermittently adjusting the center-to-center waveguide spacing along x -axis Δx .

II. THE MODEL

We consider a 2D array comprised by N quadrimer waveguides, whose single quadrimer is coupled by a PT -metric dimer and a periodically modulated dimer, see Fig.1. Within a tight-binding model with nearest-neighbor couplings, light dynamics in the optical structure along the propagation axis z are described by the following coupled-mode equation

$$i \frac{\partial \psi(z)}{\partial z} = H_N(z) \psi(z), \quad (1)$$

with the Hamiltonian

$$H_N(z) = \begin{pmatrix} h_1 & \sigma_+ & 0 & \cdots & 0 & 0 & 0 \\ \sigma_- & h_2 & \sigma_+ & 0 & \cdots & 0 & 0 \\ 0 & \sigma_- & h_3 & \sigma_+ & 0 & \cdots & 0 \\ \vdots & \ddots & \ddots & \ddots & \ddots & \ddots & \vdots \\ 0 & \cdots & 0 & \sigma_- & h_{N-2} & \sigma_+ & 0 \\ 0 & 0 & \cdots & 0 & \sigma_- & h_{N-1} & \sigma_+ \\ 0 & 0 & 0 & \cdots & 0 & \sigma_- & h_N \end{pmatrix}, \quad (2)$$

where

$$h_n = \begin{pmatrix} i\gamma & \nu & 0 & \kappa \\ \nu & -i\gamma & \kappa & 0 \\ 0 & \kappa & -A\sin(\omega z) & \nu \\ \kappa & 0 & \nu & A\sin(\omega z) \end{pmatrix}, \quad (3)$$

$$\sigma_- = \begin{pmatrix} 0 & 0 & 0 & \kappa_1 \\ 0 & 0 & \kappa_1 & 0 \\ 0 & 0 & 0 & 0 \\ 0 & 0 & 0 & 0 \end{pmatrix}, \quad \sigma_+ = \begin{pmatrix} 0 & 0 & 0 & 0 \\ 0 & 0 & 0 & 0 \\ 0 & \kappa_1 & 0 & 0 \\ \kappa_1 & 0 & 0 & 0 \end{pmatrix}.$$

Here $\psi(z) = (\psi_1(z), \psi_2(z), \psi_3(z), \dots, \psi_N(z))^T$ with $\psi_n(z) = (c_n^{(1)}(z), c_n^{(2)}(z), c_n^{(3)}(z), c_n^{(4)}(z))^T$, and $c_n^{(j)}(z)$ is the complex field amplitude in the j th waveguide of n th quadrimer for $j = 1, 2, 3, 4$ and $n = 1, 2, 3, \dots, N$. The diagonal blocks h_n describe isolated quadrimers, and the off-diagonal block matrix σ_{\pm} describe the coupling between two nearest quadrimers, where γ is the gain/loss parameter, A is the modulation amplitude and ω is the modulation frequency. The intra-dimer coupling strength is ν , which can be tuned by adjusting the distance between the waveguides along y -axis Δy . The intra-quadrimer coupling strength κ and the inter-quadrimer coupling strength κ_1 can be tuned by intermittently adjusting the distance between the waveguides along x -axis Δx [49]. Without loss of generality, we choose $\nu = 1$ to set the energy scale. To simplify, we will set all the parameters are dimensionless throughout this paper.

Under PBC, by implementing a Fourier transform

$$\begin{aligned} c_n^{(1)} &= \frac{1}{\sqrt{N}} \sum_q e^{iq(4n-3)} c_{1,q}, \\ c_n^{(2)} &= \frac{1}{\sqrt{N}} \sum_q e^{iq(4n-2)} c_{2,q}, \\ c_n^{(3)} &= \frac{1}{\sqrt{N}} \sum_q e^{iq(4n-1)} c_{3,q}, \\ c_n^{(4)} &= \frac{1}{\sqrt{N}} \sum_q e^{iq(4n)} c_{4,q}, \end{aligned}$$

one can obtain the Hamiltonian in momentum space

$$H_q(z) = \begin{bmatrix} i\gamma & \nu e^{iq} & 0 & \kappa_a \\ \nu e^{-iq} & -i\gamma & \kappa_b^* & 0 \\ 0 & \kappa_b & -A \sin(\omega z) & \nu e^{iq} \\ \kappa_a^* & 0 & \nu e^{-iq} & A \sin(\omega z) \end{bmatrix}, \quad (4)$$

where $\kappa_a = \kappa e^{i3q} + \kappa_1 e^{-iq}$, $\kappa_b = \kappa e^{-iq} + \kappa_1 e^{i3q}$ and q denotes quasi-momentum. Our system also can be regarded as two-coupled non-Hermitian SSH chains with periodical modulation or a periodically modulated non-Hermitian SSH₄ model with long rang coupling. Obviously, our system has two types of periodic character, the transverse periodic structure along x -axis and longitudinal periodic modulation along z -axis [48]. Meanwhile, its Hamiltonian is characterized by two types of the PT symmetry, the local and global ones. We say that the system is locally PT -symmetric if the isolated quadrimer is PT -symmetric in the limit $\kappa_1 = 0$. Obviously, the Hamiltonian $H_1(z)$ is PT -symmetric due to $[H_1(z), PT] = 0$, where P is a space-reversal linear operator

$$P = \begin{pmatrix} 0 & 1 & 0 & 0 \\ 1 & 0 & 0 & 0 \\ 0 & 0 & 0 & 1 \\ 0 & 0 & 1 & 0 \end{pmatrix},$$

and time operator T reverses the propagation direction: $T: i \rightarrow -i, z \rightarrow -z$. On the other hand, we say that the system is globally PT -symmetric if the infinite array (1) with the matrix $H_q(z)$ in (4) is PT -symmetric for $\kappa_1 \neq 0$ [8, 26]. The array in Fig. 1 consists of quadrimers which have unbroken local PT symmetry, at least for small γ .

III. BOUNDARY INDUCED GLOBAL PT -SYMMETRY-BREAKING

In this section, we show how the boundary, system size and inter-quadrimer coupling affect the global PT symmetry of the system. In subsection A, we show how to obtain the phase diagram via analyzing the eigenvalues of system under PBC and OBC. In subsection B, we show the energy spectra and dynamics in the three typical phases: RPT, BIPT, and BPT phases.

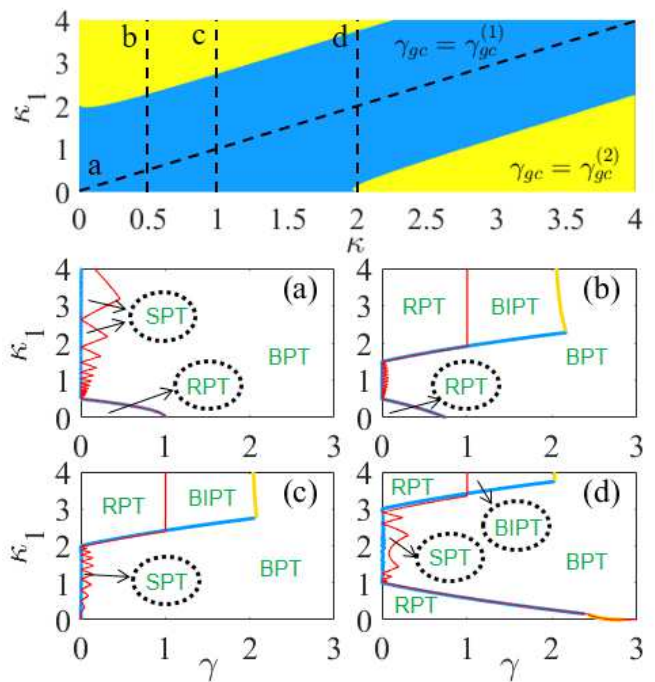


Figure 2. (Color online) (Upper) Selection of the conditions $\gamma_{gc}^{(1)}$ and $\gamma_{gc}^{(2)}$ in the parameter plane (κ, κ_1) . Phase diagram for the system in the parameter plane (γ, κ_1) for (a) $\kappa = \kappa_1$, (b) $\kappa = 0.5$, (c) $\kappa = 1$ and (d) $\kappa = 2$. Light blue and yellow lines are analytical results obtained by the formula (6) under PBC and red lines are numerical results obtained from the Hamiltonian (2) under OBC. The other parameters are chosen as $N = 20$, $A = 0$ and $\nu=1$.

A. Phase diagram

We use the usual unmodulated system as a reference system. For $A = 0$, the eigenvalues can be given as

$$E = \pm \sqrt{D + \nu^2 - \frac{\gamma^2}{2} \pm \frac{1}{2} \sqrt{4D(4\nu^2 - \gamma^2) + \gamma^4}}, \quad (5)$$

with $D = \kappa^2 + \kappa_1^2 + 2\kappa\kappa_1 \cos(4q)$ and $q \in [-\frac{\pi}{4}, \frac{\pi}{4}]$. Then the critical value of global PT -symmetry-breaking transition is determined by below conditions:

$$\gamma_{gc} = \begin{cases} \pm(D - \nu^2)/\nu; \\ \pm \sqrt{2D - 2\sqrt{D^2 - 4D\nu^2}}. \end{cases} \quad (6)$$

To distinguish, we label $\gamma_{gc}^{(1)} = |(D - \nu^2)/\nu|$ and $\gamma_{gc}^{(2)} = \left| \sqrt{2D - 2\sqrt{D^2 - 4D\nu^2}} \right|$. The selection of the conditions $\gamma_{gc}^{(1)}$ and $\gamma_{gc}^{(2)}$ in the parameter plane (κ, κ_1) is given in Fig. (2). Since the system is invariant under the transformation $\kappa_1 \leftrightarrow \kappa$ under PBC, below we will consider the case of fixing $\kappa \leq 2$ and increasing κ_1 . The intersection point between two conditions is determined by

$$4\nu^2(\kappa_1 + \kappa)^2 = \frac{[(\kappa_1 - \kappa)^2 - \nu^2]^4}{[(\kappa_1 - \kappa)^2 - \nu^2]^2 - 4\nu^4}. \quad (7)$$

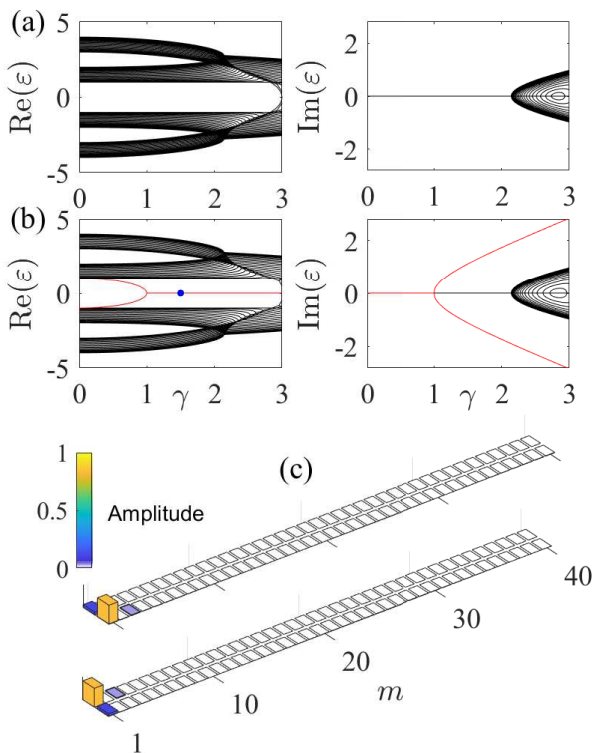


Figure 3. (Color online) (a) and (b) Real and imaginary parts of the eigenvalues as a function of γ for system under PBC (top) and OBC (bottom). (c) Representative eigenstates of zero-energy at $\gamma = 1.5$ (blue dot in (b)). The other parameters are $A = 0$, $\kappa_1 = 2.5$, $\kappa = 0.5$, $N = 20$ and $\nu = 1$.

For a fixed κ , the Eq. (7) may have several real roots. To analyze, we define the biggest genuine solution of Eq. (7) as κ_1^I . Therefore for $\kappa \leq 2$, when $\kappa_1 < \kappa_1^I$ the critical value of global PT -symmetry-breaking transition is determined by condition $\gamma_{gc}^{(1)}$. When $\kappa_1 \geq \kappa_1^I$, the critical value of global PT -symmetry-breaking transition is determined by condition $\gamma_{gc}^{(2)}$, as shown in Fig. (2). It is important to note that the limited value of $\gamma_{gc}^{(2)}$ always approach to 2 as the increases of κ_1 . Therefore, the maximal critical value of global PT -symmetry-breaking transition under PBC can be restored to $\gamma_{gc} \simeq 2$ by increasing κ_1 . In addition, as shown in Refs. [29], our unmodulated system under OBC can support the pairs of degenerate eigenstates that are the symmetric and anti-symmetric superpositions of two identical well-localized states centered symmetrically near the opposite boundaries of the system, and these pairs form effective dimers, exactly as the single PT -symmetric dimer with the critical value $\gamma_c = 1$. Therefore, the maximal critical value of global PT -symmetry-breaking transition under OBC only can be restored to $\gamma_{gc} = 1$ by increasing κ_1 . This implies that global PT symmetry of system under OBC is broken, whereas it still is unbroken under PBC for certain parameter κ_1 , and hence the boundary can induce global PT -symmetry-breaking. By setting $\gamma_{gc}^{(1)} = 1$, the criti-

cal point of boundary influencing global PT -symmetry is given as

$$\kappa_1^c = -\kappa \cos(4q) + \frac{1}{2} \sqrt{-2\kappa^2 + 4\nu + 4\nu^2 + 2\kappa^2 \cos(8q)}. \quad (8)$$

Therefore, the condition of the boundary influencing global PT symmetry is $\kappa_1 \geq \kappa_1^c$ and $1 \leq \gamma \leq 2$. For $\nu = 1$, the condition becomes $\kappa_1 \geq \kappa + \sqrt{2}$ and $1 \leq \gamma \leq 2$.

The above results indicate that for a fixed κ , depending on values of κ_1 and γ , four different situations are possible: i) robust global- PT -symmetry (RPT), where global PT -symmetries are unbroken both under PBC and OBC; ii) boundary influencing global- PT -symmetry (BIPT), where global PT symmetry is broken under OBC, whereas it still is unbroken under PBC; iii) system size affecting global- PT -symmetry (SPT), where global PT symmetry is unbroken under OBC, whereas it is broken under PBC; iv) broken global- PT -symmetry (BPT), where global PT symmetries are broken both under PBC and OBC. We show the phase diagram of global PT symmetry in the parameter plane (γ, κ_1) for different parameters κ in Fig.2 (a)-(d). For the homogeneous coupling case of $\kappa_1 = \kappa$, due to there is not boundary effect, there does not exist BIPT phase. In addition, because the limited value of $\gamma_{gc}^{(1)}$ and $\gamma_{gc}^{(2)}$ always approach to zero as the increases of κ_1 for $\kappa = \kappa_1$, the global PT symmetry always is destroyed by increasing κ_1 . Thus, the phase space (γ, κ_1) can be divided into three domains consisting of RPT, SPT and BPT as shown in Fig.2 (a). For inhomogeneous coupling case of $\kappa \neq \kappa_1$, the phase space (γ, κ_1) can be divided into multiple domains consisting of RPT, BIPT, SPT and BPT as shown in Figs.2 (b)-(d). A important feature of the phase diagram is the existence of the triple point that correspond to values $(\gamma = 1, \kappa_1 = \kappa + \sqrt{2})$, where three phases of RPT, BIPT and BPT touch. Thus depending on how parameters γ and κ_1 change in vicinity of the triple point, breaking of global PT symmetry can occur in two different ways: RPT \rightarrow BPT, or RPT \rightarrow BIPT \rightarrow BPT. Depending on the critical value of spontaneous local PT -symmetry-breaking transition γ_{lc} , which is relation to the ration of $\pm(\nu^2 - \kappa^2)/\nu$, the domain of RPT phase under parameter region of $\kappa_1 < \kappa$ and $\gamma < \gamma_{lc}$ shrinks with the increase of κ for $\kappa < \nu$ and enlarges with the increase of κ for $\kappa > \nu$ [Figs.2 (b) and 2(d)]. In particular, it disappears at $\kappa = \nu$ [Fig.2 (c)].

B. The energy spectra and dynamics in the different phases

To see clearly how the spectra change in different phases with the increase of γ , we show the real and imaginary parts of the eigenvalues as a function of γ for the system under PBC and OBC. A typical example is displayed in Figs. 3 by choosing $\kappa = 0.5$ and $\kappa_1 = 2.5$, which can undergo two phase transitions from RPT phase to

BIPT phase and from BIPT phase to BPT phase as γ continuously increase. It is clear that in the RPT phase the system has a purely real spectrum when $\gamma < 1$, however under OBC, a pair of isolated edge states with real spectrum begin to emerge when $\gamma \geq 0.5$. After undergoing a phase transition from RPT phase to BIPT phase at $\gamma = 1$, the real parts of the eigenvalues of this pair of edge states twofold degenerate zero-energy level, meanwhile its imaginary parts split into one pair of conjugated imaginary values with nonzero. Therefore, in the BIPT phase, there exists a pair of isolated zero-energy edge states with purely imaginary energy eigenvalues localized at the left boundary, whereas other $4N - 2$ eigenvalues of bulk states are real, see Fig. 3(b). Therefore, the essence of the first phase transition from RPT phase to BIPT phase is the transition of a pair of edge states of the system from real eigenvalues to complex eigenvalues. For convenience, we define this critical value as γ_{gc}^e . This is why the boundary can break global PT symmetry in our system. Of course, a pair of isolated edge states with purely real energy eigenvalues localized at the right boundary also can occur with the increase of κ_1 , but they are not zero-energy. After undergoing second phase transition from BIPT phase to BPT phase at $\gamma \simeq 2$, the real parts of $4N - 2$ ($4N$ under PBC) eigenvalues of bulk states begin to degenerate, meanwhile their imaginary parts begin to split into many pair of conjugated imaginary values with nonzero. Therefore, the essence of the second phase transition from BIPT phase to BPT phase is the transition of bulk states of the system from real eigenvalues to complex eigenvalues. Similarly, we define this critical value as γ_{gc}^b .

Through numerical integration, we analyze the light propagations of the coupled-mode system (1) in three different phases with $N = 20$. The light propagation sensitively depends upon the eigenvalues. Stationary light propagations of bounded intensity oscillations appear if all eigenvalues are real. Local light propagations of unbounded intensity oscillations appear if at least one of the eigenvalues is complex. To do this, we firstly define the light intensities in above row waveguides $I_m^a = |c_n^j(z)|^2$ for $m = 1, 2, 3, \dots, 2N$, $n = 1, 2, 3, \dots, N$ and $j = 1$, and 4, where $I_m^a = |c_n^1(z)|^2$ for m equaling odd, and $I_m^a = |c_n^4(z)|^2$ for m equaling even. Similarly, the light intensities in below row waveguides are defined as $I_m^b = |c_n^j(z)|^2$ for $j = 2$, and 3, where $I_m^b = |c_n^2(z)|^2$ for m equaling odd, and $I_m^b = |c_n^3(z)|^2$ for m equaling even. In Fig. 4, we give the light propagation using single-site excitation of away from the edge waveguide. If we choose parameters in RPT phase, the light always diffracts irrespectively of its input cell, see the left column in Fig. 4. If we choose parameters in BIPT phase, local light propagating along the edge route appear at the left edge of system, see the middle column in Fig. 4. The local light propagating along the left edge route is a direct signature of the BIPT phase. This implies that our system can be used to realize single edge-mode lasing or robust one-way edge mode transport [10]. If we choose param-

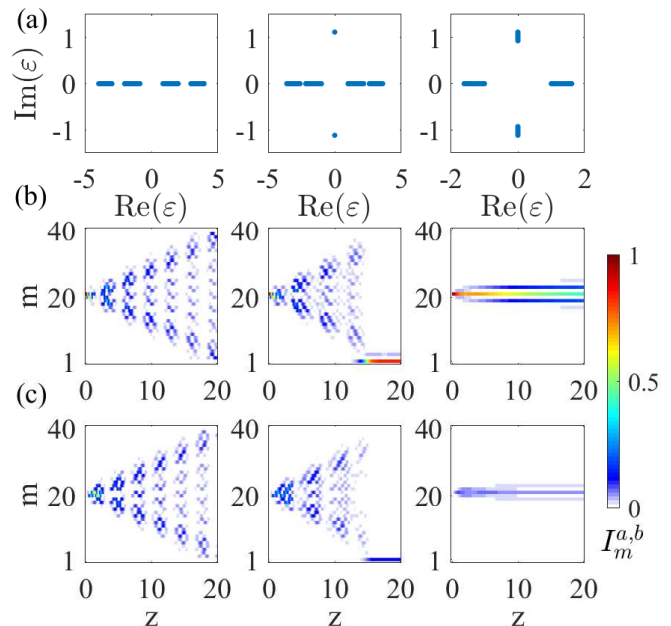


Figure 4. (Color online) (Upper) Eigenvalues distribution in the complex-energy plane. The wave packet evolution in above (middle) and below (bottom) row waveguides, respectively. In the left column we choose parameters in RPT phase, such as $\kappa = 0.5$, $\kappa_1 = 2.5$ and $\gamma = 0.5$. In the middle column we choose parameters in BIPT phase, such as $\kappa = 0.5$, $\kappa_1 = 2.5$ and $\gamma = 1.5$. In the right column we choose parameters in BPT phase, such as $\kappa = 0.5$, $\kappa_1 = 0.5$ and $\gamma = 1.5$. The other parameters are chosen as $N = 20$ and $\nu = 1$.

ters in BPT phase, the light propagating always localize at its input cell, and propagate with unbounded intensity oscillations, see the right column in Fig. 4. Therefore, our numerical simulations of the coupled-mode system (1) perfectly confirm the BIPT phase predicted by our analytical results.

IV. MANIPULATION OF GLOBAL PT SYMMETRY

In this section, we will explore how to manipulate the global PT symmetry via the periodic modulation. According to the Floquet theorem, similar to the Bloch states, the Floquet states of the modulated system (1) satisfy $\{\psi_1(z), \psi_2(z), \psi_3(z), \dots, \psi_n(z)\} = e^{-i\epsilon z} \{\tilde{\psi}_1(z), \tilde{\psi}_2(z), \tilde{\psi}_3(z), \dots, \tilde{\psi}_n(z)\}$. Here, the propagation constant ϵ is called the quasienergy, and the complex amplitudes $\tilde{\psi}_n(z)$ are periodic with the modulation period $T = 2\pi/\omega$. Then the quasienergies and eigenfunctions are given by $\mathcal{F}\tilde{\psi}_n = \epsilon\tilde{\psi}_n$, with the Floquet operator $\mathcal{F} = -i\frac{d}{dz} + H_N(z)$. Under high-frequency Floquet analysis, the correspondingly effective Hamiltonian can be

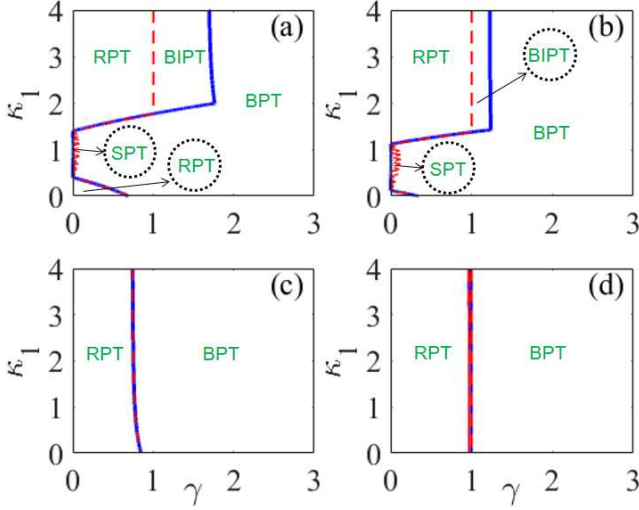


Figure 5. (Color online) Phase diagram of the system in the parameter plane (γ, κ_1) for different modulation parameters (a) $A/\omega = 0.6$, (b) $A/\omega = 1$, (c) $A/\omega = 1.5$ and (d) $A/\omega = 2.4$. Blue lines are numerical results obtained from the Hamiltonian (9), and red lines are numerical results obtained from the Hamiltonian (2). The other parameters are chosen as $N = 20$, $\kappa = 0.5$, $\omega = 10$ and $\nu = 1$.

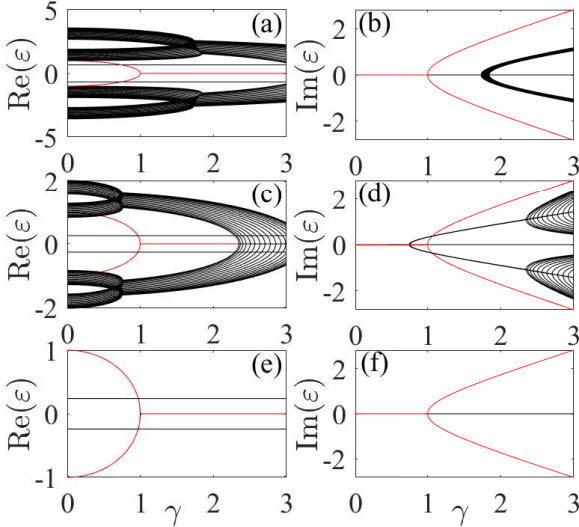


Figure 6. (Color online) Real and imaginary parts of the quasienergies of the system under OBC as a function of γ for $A/\omega = 0.6$ (top), 1.5 (middle) and 2.4 (bottom). The other parameters are $\omega = 10$, $\kappa_1 = 2.5$, $\kappa = 0.5$, $N = 20$ and $\nu = 1$.

written as

$$H_q^{eff} = \begin{bmatrix} i\gamma & \nu e^{iq} & 0 & \kappa_a \tilde{J} \\ \nu e^{-iq} & -i\gamma & \kappa_b^* \tilde{J}^* & 0 \\ 0 & \kappa_b \tilde{J} & 0 & \nu e^{iq} \tilde{Q} \\ \kappa_a^* \tilde{J}^* & 0 & \nu e^{-iq} \tilde{Q}^* & 0 \end{bmatrix}, \quad (9)$$

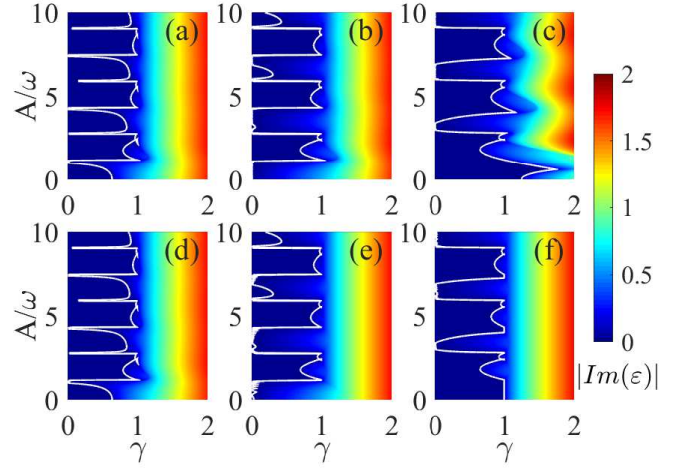


Figure 7. (Color online) The imaginary parts of the quasienergies $|Im(\varepsilon)|$ as a function of A/ω and γ under PBC (top) and OBC (bottom) with different coupling strengths $\kappa_1 = 0.1$ (left), $\kappa_1 = 1$ (middle) and $\kappa_1 = 2$ (right). The other parameters are chosen as $N = 20$, $\kappa = 0.5$, $\omega = 10$ and $\nu = 1$.

with

$$\tilde{J} = \sum_{k=-\infty}^{\infty} (i)^k J_k(A/\omega) e^{ik\omega z},$$

$$\tilde{Q} = \sum_{k=-\infty}^{\infty} (i)^k J_k(2A/\omega) e^{ik\omega z}.$$

The modulus of \tilde{J} and \tilde{Q} depend on the values of A/ω , and can change between zero and one. In particular, the modulus $|\tilde{J}|$ equals zero at some specific values of A/ω (such as $A/\omega \simeq 2.4$ and 5.52), and the modulus $|\tilde{Q}|$ equals zero at $A/\omega \simeq 1.2$ and 2.76 . Then the spectra ε are given by the roots of the secular equation

$$\varepsilon^4 + [\gamma^2 - \nu^2(1 + \tilde{Q}^2) - \tilde{J}^2(|\kappa_a|^2 + |\kappa_b|^2)]\varepsilon^2 + i\gamma\tilde{J}^2(|\kappa_b|^2 - |\kappa_a|^2)\varepsilon - \tilde{J}^2\nu^2\tilde{Q}e^{-i2q}(\kappa_a\kappa_b + \kappa_a^*\kappa_b^*) + (\nu^4 - \gamma^2\nu^2)\tilde{Q}^2 + \tilde{J}^4|\kappa_a|^2|\kappa_b|^2 = 0. \quad (10)$$

From Eq. (10), we can see for a fixed γ , κ and κ_1 , the spontaneous global PT -symmetry-breaking transition can be manipulated by tuning modulation parameter, because the modulus $|\tilde{J}|$ and $|\tilde{Q}|$ periodically change from zero to one along with the modulation parameter A/ω . For the special value $\tilde{J} = 0$, the quasienergies become as $\varepsilon = \pm\tilde{Q}\nu$ and $\pm\sqrt{\nu^2 - \gamma^2}$, and the critical value of global PT -symmetry-breaking transition is $\gamma_{gc} = \nu$. In this situation, the system decouples N uncoupled PT -symmetric dimers, and hence the critical value of PT -symmetry-breaking transition is determined by single PT -symmetric dimer. For the the special value $\tilde{Q} = 0$, the quasienergies become as

$$\varepsilon = \pm \sqrt{\frac{2D\tilde{J}^2 + \Gamma \pm \sqrt{\Gamma(4D\tilde{J}^2 + \Gamma)}}{2}},$$

with $\Gamma = \nu^2 - \gamma^2$. The critical value of global PT -symmetry-breaking transition is $\gamma_{gc} = \nu$. Therefore, for the special values $\tilde{J} = 0$ or $\tilde{Q} = 0$, the critical value of global PT -symmetry-breaking transition $\gamma_{gc} = \nu = 1$ is independent of parameters κ , κ_1 and boundary condition. Then in the parametric region $\kappa_1 > \kappa + \sqrt{2}$ and $1 < \gamma \leq 2$, the critical value γ_{gc}^b is adjusted from 2 to 1, as A/ω increases from 0 to 1.2. Furthermore, the critical value γ_{gc}^b can be adjusted to less than 1 for $1.2 < A/\omega < 2.4$. This implies that the domain of the BIPT phase can be manipulated narrow and even disappeared by tuned A/ω .

To verify above analytical results, we show the phase diagram of global PT symmetry in the parameter plane (γ, κ_1) for different modulation parameters A/ω in Fig.5. As an example, we choose the unmodulated case in Fig.2 (b) as a reference system. Obviously, the presence of periodic modulation modifies previous physical picture. Firstly, it clearly shows that the domain of the BIPT phase can be manipulated narrow and even disappeared by tuning A/ω , and hence the triple point also vanish. Second, the domain of BPT phase under parameter region of $\kappa_1 < \kappa + \sqrt{2}$ and $\gamma < 1$ can be adjusted RPT phase with the increase of A/ω . Then the phase space (γ, κ_1) only can be divided into two domains consisting of RPT and BPT for $1.2 \leq A/\omega \leq 2.4$, where the critical value γ_{gc} not only is independent of parameters κ and κ_1 , but also independent of boundary condition, as shown in Figs.5(c) and (d). To see clearly how the spectra change in different phases with the increase of γ for different modulation parameters A/ω , we show the real and imaginary parts of the quasienergies as a function of γ for the system under OBC. A typical example is displayed in Figs. 6 by choosing modulation parameters $A/\omega = 0.6, 1.5$ and 2.4 . It is clearly show that the critical value γ_{gc}^e is independent of modulation parameter A/ω , but the critical value γ_{gc}^b can be adjusted small by tuning A/ω . The critical value γ_{gc}^b change from 2 to 1 as A/ω increases from 0 to 1.2, and γ_{gc}^b can be adjusted to less than 1 for $1.2 < A/\omega < 2.4$. Therefore, when $\gamma_{gc}^b \leq \gamma_{gc}^e$ for $1.2 \leq A/\omega \leq 2.4$, a pair of isolated zero-energy edge states embed into bulk states, and then the BIPT phase disappears. This is why BIPT phase can be manipulated by tuning modulation parameter in our system.

To show the parameter dependence of global PT symmetry from another angle, we show the quasienergies $|Im(\varepsilon)|$ as a function of A/ω and γ for different coupling parameters (κ, κ_1) both for PBC and OBC. As an example, we choose three sets of coupling parameters that initially be in RPT phase ($\kappa = 0.5, \kappa_1 = 0.1$), BPT phase ($\kappa = 0.5, \kappa_1 = 1$) and BIPT phase ($\kappa = 0.5, \kappa_1 = 2$), as shown in Fig.7. It is clearly see that whether or not the system has initial global PT symmetry, the periodic modulation not only can restore the broken global PT symmetry, but also can control it by tuning modulation amplitude. Differently, the global PT -symmetry only can be adjusted to the critical value $\gamma_{gc} = 1$ for parametric

region that initially be in RPT phase, BPT phase and BIPT phase of the system under OBC, whereas it can be adjusted to $\gamma_{gc} > 1$ for parametric region that initially be in BIPT phase of the system under PBC. Therefore, for our modulated system of fixed γ , it is possible to observe the spontaneous global PT -symmetry-breaking transition by tuning A/ω . It is important to note that the global property of transverse periodic structure of such a 2D optical array can be manipulated by only tuning modulation amplitude of longitudinal periodic modulation.

V. CONCLUSION AND DISCUSSION

In summary, we have investigated the static and dynamical property of global PT symmetry in 2D arrays of periodically modulated PT -symmetric quadrimer waveguides. For unmodulated case with inhomogeneous inter- and intra- quadrimer coupling strength $\kappa_1 \neq \kappa$, in addition to conventional global PT -symmetric phases and PT -symmetry-breaking phase, we find that there is exotic phase where global PT symmetry is broken under OBC, whereas it still is PT -symmetric under PBC. The boundary of phase is analytically given as $\kappa_1 \geq \kappa + \sqrt{2}$ and $1 \leq \gamma \leq 2$, where there exists a pair of zero-energy edge states with purely imaginary energy eigenvalues localized at the left boundary, whereas other $4N - 2$ eigenvalues are real. The parametric dependence of the spontaneous global PT -symmetry-breaking is analytically and numerically explored for the modulated array. Because critical value γ_{gc}^e is independent of modulation parameter A/ω , and the critical value γ_{gc}^b can be adjusted small by tuning A/ω , the domain of the BIPT phase can be manipulated narrow and even disappeared by tuning A/ω . More interestingly, whether or not the array has initial global PT symmetry, periodic modulation not only can restore the broken global PT symmetry, but also can control it by tuning modulation amplitude. Therefore, the global property of transverse periodic structure of a 2D optical array can be manipulated by only tuning modulation amplitude of longitudinal periodic modulation. Our results provide a promising approach for designing and manipulating optical material and may have specific technological importance.

With currently available techniques, it is possible to realize our model and observe our theoretical predictions with experiments. Our proposed structure can be demonstrated experimentally in numerous optical systems [9, 13, 50]. For instance, in photonics, one can use the femtosecond direct writing method [52] to realize a 2D array of PT -symmetric photonic coupled waveguide. Periodic modulations can be introduced by harmonic modulations of the real refractive index or periodic curvatures along the propagation direction [53–55]. For such a 2D optical array with periodic modulation, spontaneous global PT -symmetry-breaking transition may be observed by adjusting the modulation parameter. In ad-

dition, it is also possible to apply our model and method for designing some optical devices, such as single edge-mode laser and robust one-way edge mode transport.

ACKNOWLEDGMENTS

H. Zhong is thankful to Chaohong Lee for enlightening suggestions and helpful discussions. This work is sup-

ported by the National Natural Science Foundation of China under Grant No. 11805283 and No. 11725417, the Hunan Provincial Natural Science Foundation under Grants No. 2019JJ30044, and the Talent project of Central South University of Forestry and Technology under Grant No. 2017YJ035.

-
- [1] V. V. Konotop, J. Yang, and D. A. Zezyulin, Nonlinear waves in PT-symmetric systems, *Rev. Mod. Phys.* 88, 035002 (2016).
- [2] C. M. Bender, PT Symmetry (World Scientific, Singapore, 2019); D. Christodoulides and J. Yang, Parity-Time Symmetry and Its Applications (Springer, Berlin, 2018).
- [3] N. Moiseyev, Non-Hermitian Quantum Mechanics (Cambridge, 2011).
- [4] R. El-Ganainy, K. G. Makris, M. Khajavikhan, Z. H. Musslimani, S. Rotter and D. N. Christodoulides, Non-Hermitian physics and PT symmetry, *Nat. Phys.* 14, 11(2018).
- [5] C. M. Bender and S. Boettcher, Real Spectra in Non-Hermitian Hamiltonians Having PT Symmetry, *Phys. Rev. Lett.* 80, 5243 (1998).
- [6] C. M. Bender, Making Sense of non-Hermitian Hamiltonians, *Rept. Prog. Phys.* 70, 947 (2007).
- [7] S. V. Suchkov, A. A. Sukhorukov, J. Huang, S. V. Dmitriev, C. Lee, and Y. S. Kivshar, Nonlinear switching and solitons in PT-symmetric photonic systems, *Laser Photon. Rev.* 10, 177 (2016).
- [8] C.V. Morfonios, P.A. Kalozoumis, F.K. Diakonov and P. Schmelcher, Nonlocal discrete continuity and invariant currents in locally symmetric effective Schrödinger arrays, *Annals of Physics* 385, 623 (2017).
- [9] S. Weimann, M. Kremer, Y. Plotnik, Y. Lumer, S. Nolte, K. G. Makris, M. Segev, M. C. Rechtsman, and A. Szameit, Topologically protected bound states in photonic parity-time-symmetric crystals, *Nat. Mater.* 16, 433 (2017).
- [10] M. Parto, S. Wittek, H. Hodaei, G. Harari, M. A. Bandres, J. Ren, M. C. Rechtsman, M. Segev, D. N. Christodoulides, and M. Khajavikhan, Edge-Mode Lasing in 1D Topological Active Arrays, *Phys. Rev. Lett.* 120, 113901 (2018).
- [11] N. X. A. Rivolta, H. Benisty and B. Maes, Topological edge modes with PT symmetry in a quasiperiodic structure, *Phys. Rev. A* 96, 023864 (2017).
- [12] L. Ge, Y. D. Chong, and A. D. Stone, Conservation relations and anisotropic transmission resonances in one-dimensional PT-symmetric photonic heterostructures, *Phys. Rev. A* 85, 023802 (2012).
- [13] A. Regensburger, C. Bersch, M.-A. Miri, G. Onishchukov, D. N. Christodoulides and U. Peschel, Parity-time synthetic photonic lattices, *Nature (London)* 488, 167 (2012).
- [14] Z. Gao, S. T. M. Fryslie, B. J. Thompson, P. S. Carney, and K. D. Choquette, Parity-time symmetry in coherently coupled vertical cavity laser arrays, *Optica* 4, 323 (2017).
- [15] D. J. Nodal Stevens, B. Jaramillo Ávila, and B. M. Rodríguez-Lara, Necklaces of PT-symmetric dimers, *Photonics Research* 6, A31 (2018).
- [16] S. Longhi, Convective and absolute PT-symmetry breaking in tight-binding lattices, *Phys. Rev. A* 88, 052102 (2013).
- [17] C. M. Bender, M. Gianfreda, and S. P. Klevansky, Systems of coupled PT-symmetric oscillators, *Phys. Rev. A* 90, 022114 (2014).
- [18] D. A. Zezyulin and V. V. Konotop, Nonlinear Modes in Finite-Dimensional PT-Symmetric Systems, *Phys. Rev. Lett.* 108, 213906 (2012).
- [19] S. Longhi, PT phase control in circular multi-core fibers, *Opt. Lett.* 41, 1897 (2016).
- [20] S. V. Dmitriev, A. A. Sukhorukov and Y. S. Kivshar, Binary parity-time-symmetric nonlinear lattices with balanced gain and loss, *Opt. Lett.* 35, 2976 (2010).
- [21] X. M. Yang, X. Z. Zhang, C. Li and Z. Song, Dynamical signature of the moiré pattern in a non-Hermitian ladder, *Phys. Rev. A* 98, 085306 (2018).
- [22] H. Ramezani, T. Kottos, V. Kovanic and D. N. Christodoulides, Exceptional-point dynamics in photonic honeycomb lattices with PT symmetry, *Phys. Rev. A* 85, 013818 (2012).
- [23] I. V. Barashenkov, L. Baker and N. V. Alexeeva, PT-symmetry breaking in a necklace of coupled optical waveguides, *Phys. Rev. A* 87, 033819 (2013).
- [24] H. Ramezani, Non-Hermiticity-induced flat band, *Phys. Rev. A* 96, 011802(R) (2017).
- [25] P. A. Kalozoumis, C. V. Morfonios, F. K. Diakonov, and P. Schmelcher, PT-symmetry breaking in waveguides with competing loss-gain pairs, *Phys. Rev. A* 93, 063831 (2016).
- [26] V. V. Konotop, D. E. Pelinovsky, and D. A. Zezyulin, Discrete solitons in PT-symmetric lattices, *Europhys. Lett.* 100, 56006 (2012).
- [27] N. V. Alexeeva, I. V. Barashenkov and Y. S. Kivshar, Solitons in PT-symmetric ladders of optical waveguides, *New J. Phys.* 19, 113032 (2017).
- [28] M. C. Zheng, D. N. Christodoulides, R. Fleischmann, and T. Kottos, PT optical lattices and universality in beam dynamics, *Phys. Rev. A* 82, 010103(R) (2010).
- [29] O. Bendix, R. Fleischmann, T. Kottos, and B. Shapiro, Optical structures with local PT-symmetry *J. Phys. A: Math. Theor.* 43, 265305 (2010).
- [30] Y. N. Joglekar, D. Scott and M. Babbey, Robust and fragile PT -symmetric phases in a tight-binding chain, *Phys. Rev. A* 82, 030103(R) (2010).

- [31] N. Bender, H. Li, F. M. Ellis and T. Kottos, Wave-packet self-imaging and giant recombinations via stable Bloch-Zener oscillations in photonic lattices with local PT symmetry, *Phys. Rev. A* 92, 041803(R) (2015).
- [32] O. Bendix, R. Fleischmann, T. Kottos and B. Shapiro, Exponentially Fragile PT Symmetry in Lattices with Localized Eigenmodes, *Phys. Rev. Lett.* 103, 030402 (2009).
- [33] B. P. Nguyen and K. Kim, Transport and localization of waves in ladder-shaped lattices with locally PT-symmetric potentials, *Phys. Rev. A* 94, 062122 (2016).
- [34] B. Zhu, R. Lü and S. Chen, PT symmetry in the non-Hermitian Su-Schrieffer-Heeger model with complex boundary potentials, *Phys. Rev. A* 89, 062102 (2014).
- [35] M. Klett, H. Cartarius, D. Dast, J. Main and G. Wunner, Relation between PT-symmetry breaking and topologically nontrivial phases in the Su-Schrieffer-Heeger and Kitaev models, *Phys. Rev. A* 95, 053626 (2017).
- [36] S. Lieu, Topological phases in the non-Hermitian Su-Schrieffer-Heeger model, *Phys. Rev. B* 97, 045106 (2018).
- [37] J. Hou, Y. J. Wu and C. Zhang, Two-dimensional non-Hermitian topological phases induced by asymmetric hopping in a one-dimensional superlattice, arXiv:1906.03988v1.
- [38] C. Yuce and Z. Oztas, PT symmetry protected non-Hermitian topological systems, *Scientific Reports* 8, 17416 (2018).
- [39] N. Moiseyev, Crossing rule for a PT-symmetric two-level time-periodic system, *Phys. Rev. A* 83, 052125 (2011).
- [40] X. Lian, H. Zhong, Q. Xie, X. Zhou, Y. Wu, and W. Liao, PT-symmetry-breaking induced suppression of tunneling in a driven non-Hermitian two-level system, *Eur. Phys. J. D* 68, 189 (2014).
- [41] Y. N. Joglekar, R. Marathe, P. Durganandini, and R. K. Pathak, PT spectroscopy of the Rabi problem, *Phys. Rev. A* 90, 040101(R) (2014).
- [42] J. Gong and Q. H. Wang, Stabilizing non-Hermitian systems by periodic driving, *Phys. Rev. A* 91, 042135 (2015).
- [43] X. Luo, J. Huang, H. Zhong, X. Qin, Q. Xie, Y. S. Kivshar, and C. Lee, Pseudo-Parity-Time Symmetry in Optical Systems, *Phys. Rev. Lett.* 110, 243902 (2013).
- [44] Z. Zhou, B. Zhu, and L. Zhang, Analytical Study on Propagation Dynamics of Optical Beam in Parity-Time Symmetric Optical Couplers, *Commun. Theor. Phys.* 63, 406 (2015).
- [45] Y. Wu, B. Zhu, S. Hu, Z. Zhou and H. Zhong, Floquet control of the gain and loss in a PT-symmetric optical coupler, *Front. Phys.* 12, 121102 (2017).
- [46] A. Y. Song, Y. Shi, Q. Lin and S. Fan, Direction-dependent parity-time phase transition and nonreciprocal amplification with dynamic gain-loss modulation, *Phys. Rev. A* 99, 013824 (2019).
- [47] M. Chitsazi, H. Li, F. M. Ellis, and T. Kottos, Experimental Realization of Floquet PT-Symmetric Systems, *Phys. Rev. Lett.* 119, 093901 (2017).
- [48] H. Benisty, A. Lupu and A. Degiron, Transverse periodic PT symmetry for modal demultiplexing in optical waveguides, *Phys. Rev. A* 91, 053825 (2015).
- [49] G. P. Agrawal, *Application of nonlinear fiber optics* (Academic Press, 2008).
- [50] C. E. Rüter, K. G. Makris, R. El-Ganainy, D. N. Christodoulides, M. Segev, and D. Kip, Observation of parity-time symmetry in optics, *Nat. Phys.* 6, 192 (2010).
- [51] A. Guo, G. J. Salamo, D. Duchesne, R. Morandotti, M. Volatier-Ravat, V. Aimez, G. A. Siviloglou, and D. N. Christodoulides, Observation of PT-Symmetry Breaking in Complex Optical Potentials, *Phys. Rev. Lett.* 103, 093902 (2009).
- [52] A. Szameit and S. Nolte, Discrete optics in femtosecond-laser-written photonic structures, *J. Phys. B: At. Mol. Opt. Phys.* 43, 163001 (2010).
- [53] S. Longhi, Quantum-optical analogies using photonic structures, *Laser Photon. Rev.* 3, 243 (2009).
- [54] I. L. Garanovich, S. Longhi, A. A. Sukhorukov, Y. S. Kivshar, Light propagation and localization in modulated photonic lattices and waveguides, *Phys. Rep.* 518, 1 (2012).
- [55] J. M. Zeuner, M. C. Rechtsman, Y. Plotnik, Y. Lumer, S. Nolte, M. S. Rudner, M. Segev, and A. Szameit, Observation of a Topological Transition in the Bulk of a Non-Hermitian System, *Phys. Rev. Lett.* 115, 040402 (2015).